

SHORT WAVELENGTH SASE FELS: EXPERIMENTS VERSUS THEORY

J. Rossbach, Universität Hamburg and DESY, 22603 Hamburg, Germany

Abstract

The basic theory of short wavelength SASE FELs is presented. Predictions are compared with experimental findings achieved primarily at FLASH, DESY.

INTRODUCTION

Free-electron lasers (FEL) operating in the SASE mode (self-amplified spontaneous emission) at wavelengths far below the visible are now with us since several years, and more, and even more ambitious, projects are ahead of us. It is thus appropriate to hold on for a moment and summarize how the experimental observations compare with theory. The present paper does this on a very basic level, i.e. only the fundamental theoretical considerations are presented, and simple models are used to explain the key physics involved. From such basic considerations, however, reasonably precise predictions can be made on almost all relevant FEL output parameters. These predictions are then readily compared with state-of-the-art experimental findings, most of which stem from FLASH at DESY/Hamburg, presently being the only SASE FEL operating in the VUV wavelength regime down to 13 Nanometers. In this respect, the paper is primarily of educative purpose (see Figure 1). However, the cumulative way of condensed presentation may also serve as a guideline for the basic design of new facilities and sheds some light on the key technical challenges.

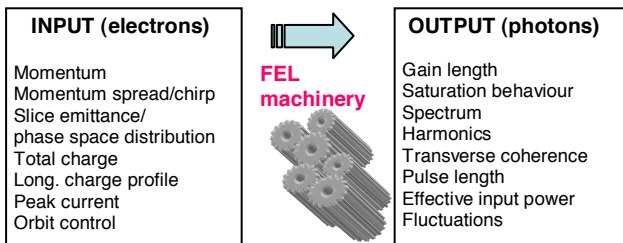


Figure 1: We consider the FEL as a machinery with input provided by the electron beam and some output given by the photon beam. Do we understand how this machinery works?

The enormous radiation power generated by an FEL is based on the fact that a “point-like” bunch of electrons radiates at a power $P_{\text{rad}} \sim N_e^2$ with N_e the number of electrons in the bunch. This is in contrast to spontaneous radiation of electrons in standard synchrotron radiation which scales linearly with N_e since electrons are uncorrelated in space and time.

In order to increase the power and the coherence of the radiation one has to force the electrons to emit coherently

by compressing them into a length small compared to the wavelength of the radiation. Such a tight compression on an entire bunch is not possible for wavelengths in the nanometer regime. However, if one succeeds to arrange a large number of “point-like” bunchlets longitudinally into a periodic array, with the periodicity given by the wavelength of radiation, one obtains indeed coherent radiation of these bunchlets with the additional advantage of compressing all the radiation into a narrow forward cone. The principle of the Free-Electron Laser (FEL) [1] is based on this idea.

BASICS OF THE HIGH-GAIN FEL

In an FEL, the density of an electron bunch is modulated with the periodicity of the radiation wavelength λ_{ph} by a resonant process taking place in the combined presence of the periodic transverse magnetic field of an undulator and an electromagnetic wave in this same magnet. In the following, the description of the FEL mechanism comes in three steps (see, e.g. [2], [3]):

1. Energy modulation.

Consider an electron moving along the axis of a planar undulator with period length λ_u . Its transverse velocity is given by

$$v_x(z) = c \frac{K}{\gamma} \cos\left(\frac{2\pi}{\lambda_u} z\right), \quad (1)$$

where $\gamma = E/(m_e c^2)$ is the relativistic factor of the electrons, and $K = eB_u \lambda_u / 2\pi m_e c$ is the “undulator parameter” with B_u being the peak magnetic field in the undulator.

The x -component of the electromagnetic wave with amplitude E_{Light} moving in z -direction is described by

$$E_x(z, t) = E_{\text{Light}} \cos(k_L z - \omega_L t) \quad (2)$$

where the indices L mean “Light”, although the wavelength is not at all restricted to the visible.

In the combined presence of (1) and (2), the electron energy W changes at a rate

$$\frac{dW}{dz} = \frac{q}{v_z} \vec{v} \cdot \vec{E} = -\frac{q E_{\text{Light}} K}{\gamma \beta_z} \sin \Psi, \quad (3)$$

with the “ponderomotive phase”

$\Psi = (k_u + k_L)z - \omega_L t + \varphi_0$. The energy lost (or taken) by the electron is taken from or transferred to the radiation field. Obviously, W can be either negative or positive, depending on the sign of $\sin \Psi$. For most wavelengths, $\sin \Psi$ oscillates very rapidly such that there is no net energy transfer. Continuous energy transfer is only possible if Ψ remains constant: $d\Psi/dz = 0$. This condition

imposes a relation between γ , K , λ_u and λ_L , the FEL resonance condition

$$\lambda_{ph} = \frac{\lambda_u}{2\gamma^2} \left(1 + \frac{K^2}{2} \right), \quad (4)$$

which is identical to the wavelength of spontaneous undulator radiation.

2. Current modulation.

If the electron energy changes (due to the process just described) by an amount $\Delta\gamma$, the electron will move away from resonance at a rate

$$\frac{d\Psi}{dz} = k_u \frac{2}{\gamma_{res}} \Delta\gamma \quad (5)$$

γ_{res} is the resonance energy.

Combining Eqs. (3) and (5) results in a pendulum equation

$$\frac{d^2\Psi}{dz^2} = -\Omega^2 \sin\Psi$$

describing phase focussing in $\Delta\gamma/\Psi$ phase plane. This is perfectly equivalent to synchrotron oscillation, with the only difference that the spatial period length is the optical wavelength λ_L . As with synchrotron oscillations, the beam rotates in phase space within the separatrix. Thus, an initially unbunched beam gets bunched. A longitudinal density modulation develops on the optical wavelength.

3. Radiation.

The generated modulation amplitude of current density is called j_{Light} . From Maxwell's equations it is well known, that a modulated current, moving on its oscillating trajectory inside the undulator, will radiate at a wavelength given by eq. (4). The rate at which the amplitude E_{Light} of the optical wave grows can be shown to be proportional to

$$\dot{j}_{Light}: \quad \frac{dE_{Light}}{dz} = const \cdot j_{Light} \quad (6)$$

Eqs. (3,5,6) represent a set of ordinary coupled first order differential equations in the variables $\Delta\gamma/\Psi$ describing most of the properties of the high-gain FEL [4,5]. It is important to realize that Eq. (6) exhibits the source of an unstable feedback behaviour: When E_{Light} increases, also the energy modulation will increase according to Eq. (3), speeding up the growth of the density modulation (Eq. (5)), etc.

Eqs. (3,5,6) can be combined into a single differential equation of third order, if additional simplifying assumptions are made. In the most simple case (1D, all particles on resonance), the complex amplitude \mathbf{E} of the light wave obeys

$$\frac{d^3\mathbf{E}}{dz^3} = i\Gamma^3\mathbf{E} \quad (7)$$

For distances $z \gg L_G$, the solution

$$P_{rad} = \frac{1}{9} P_{in} \exp\left(\frac{z}{L_G}\right) \quad (8)$$

dominates all the other solutions. The e-folding length of the power of the electromagnetic field is called (power) gain length. It is worthwhile noting, that (in our 1D approximation) its dependence on beam parameters is only given by \hat{I}/σ_r^2 , i.e. the peak current \hat{I} inside the bunch and the cross section, i.e. by the current density:

$$L_G = \frac{1}{\sqrt{3}} \left(\frac{I_A \gamma^3 \sigma_r^2 \lambda_u}{4\pi \cdot \hat{I} \cdot K^2} \right)^{1/3}, \quad (9)$$

The most important 3D effect that makes comparison with experiments difficult is the assumption made, that the transverse overlap between electron beam and radiation field is perfect, which is very difficult to verify in a realistic setup.

Eq. (8) suggests, that the exponential growth might proceed forever, however it follows from Eqs. (3,5,6) more correctly that the gain reaches saturation when the density modulation is almost complete, see Fig. 2. While the field amplitude during the exponential growth sensitively depends on the input power P_{in} , the maximum power achieved in saturation depends much less on beam parameters and is thus much better suited for a direct comparison with experiment.

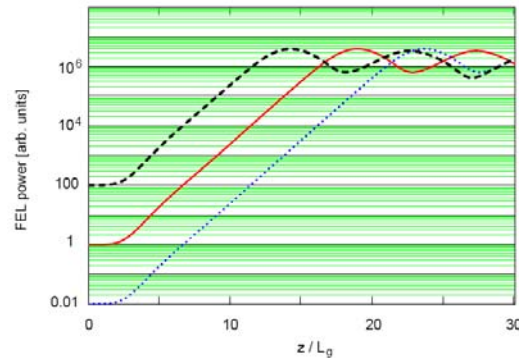


Figure 2: Basic 1D FEL theory describes both exponential growth of power and saturation behaviour. The e-folding length as well as the saturation power are rather independent from the input power level.

The gain length can be combined with the undulator period into the most important "FEL-parameter" [4]

$$\rho_{FEL} = \frac{1}{4\pi\sqrt{3}} \frac{\lambda_u}{L_G} \approx 10^{-4} \dots 10^{-2} \quad (10)$$

Experimental data from pioneering high-gain experiments are shown in Fig. 3 to agree nicely in terms of both the exponential growth of radiation power and the saturation power level. Also the measured gain length corresponds to reasonable beam parameters. It should be noted, though, that the knowledge about the beam parameters (e.g. peak current inside the bunch) is generally not precise enough as to be able to predict the gain length with high accuracy from a measurement on the electron beam.

Bandwidth

If, at the entrance of the undulator, the electrons' momenta don't perfectly match the resonance condition $q \cdot (4)$, evaluation of Eqs. (3,5,6) predicts a dramatic reduction of gain, if the momentum error $\eta_0 = \Delta p/p_0$ exceeds some critical limit given by $\eta_0 < \rho_{FEL}$. This reduction is even more pronounced if there is a momentum spread around the center momentum, see Figure 4. In consequence, the FEL can amplify only wavelengths within a narrow wavelength band:

$$|\Delta\omega|/\omega < 2\rho_{FEL} \tag{11}$$

a property that can be compared with measured spectra, see Fig. 5.

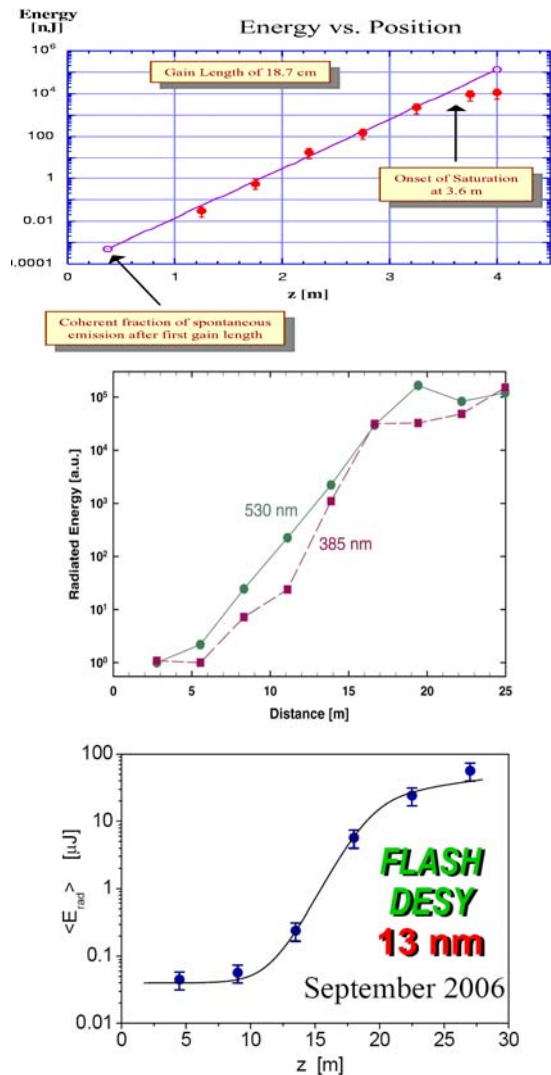


Figure 3: Demonstration of exponential growth and saturation of radiation energy at the VISA FEL at 845 nm radiation wavelength [6] (top), at LEUTL (530 nm and 385 nm, middle) [7], and at FLASH/DESY (13 nm, bottom) [8].

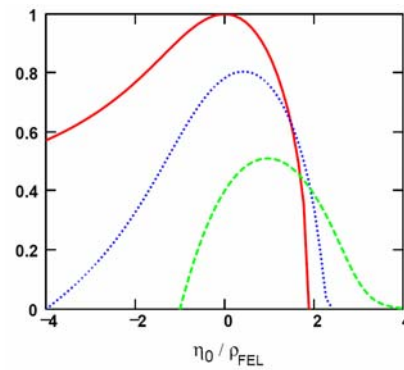


Figure 4: Dependence of the (normalized) gain on the relative deviation η_0 of the momentum from resonance. Solid red line: No momentum spread, dotted blue line: rms momentum spread $\sigma_\eta = 0.5\rho_{FEL}$, broken green line: $\sigma_\eta = 1.0\rho_{FEL}$.

Generally the agreement is very nice. A departure from Eq. (11) may arise if the FEL runs into deep saturation, if there is a large momentum chirp inside the bunch, or (in terms of averaged spectra) if the beam energy delivered by the accelerator is not stable.

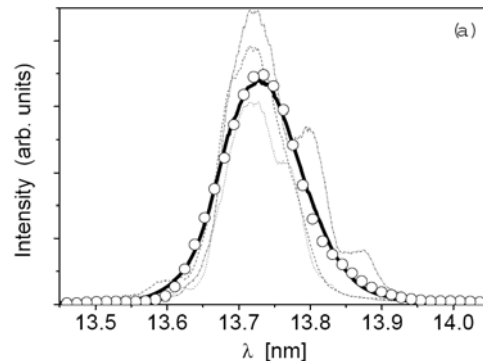


Figure 5: Several single-shot spectra (broken lines) and average spectrum (solid line), all taken at FLASH [8], and prediction by the simulation code FAST (dots) [9].

START-UP FROM NOISE

From analysis of Eqs. (3,5,6), and also from Eq. (7), it follows that exponential growth with power e-folding length L_G is not necessarily started from an initial radiation power but equally well from an initial density modulation at the resonant wavelength. Again, as in the case of input power, the real level of input modulation does not matter for finally achieving laser saturation.

For very short wavelengths, it is very difficult to generate any controlled density modulation by the accelerator. However, realizing that a random electron distribution has a white noise spectrum and thus contains some non-zero density modulation component at *any* wavelength, one concludes that an FEL will always start up from noise. This "Self-Amplified-Spontaneous Emission (SASE)" mode of operation [10] has turned out

to be a very robust mode of operation since it does not depend on the existence of any external input signal.

The interesting question arises, how powerful an input signal must be in order to dominate the start-up due to SASE that will happen anyway? Such “equivalent input power” level can be estimated analytically [2], and it is an important result of numerical SASE simulation codes. It can be compared with experiment by extrapolating the measured exponential gain curve back to the entrance of the undulator, see Fig. (6). Generally, there is a satisfactory agreement.

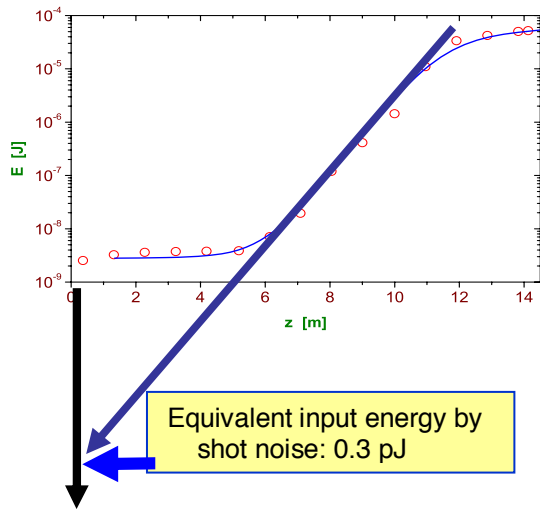


Figure 6: Experimental determination of the “equivalent input power” of the SASE process using data taken at the TTF FEL at DESY (dots) [11]. The solid curve represents result of a numerical simulation.

Fluctuations and Pulse Length

The radiation output of a SASE FEL fluctuates from shot to shot, as illustrated in Fig. 7. It is important to note that this fluctuation is not a mysterious property of the FEL amplifier, but it is just a property of the input signal, namely the spontaneous undulator radiation. This can be understood as follows.

Consider first the superposition of many wave trains with arbitrary phases (one-dimensional, length being determined by the coherence length λ_{coh} in our case, i.e. by the number of wavelengths within a gain lengths). If each wave train originating from an electron located in a bunch much shorter than the wave train, all the waves overlap in time and there is large probability for complete destructive interference. In fact, the probability distribution function is given in this case by a negative exponential: $p(E) \propto \exp(-E)dE$, as illustrated in Fig. 8a. If, in contrast, the electron bunch is considerably longer than the wave train, there is much less probability of destructive interference, since many wave trains don't overlap any more in time, see Fig. 8b. Instead, superposition in time domain results in a sequence of optical modes, each of typical length λ_{coh} . Thus, we

expect a number M of optical modes roughly given by $M \approx \text{bunch length} / \lambda_{coh}$.

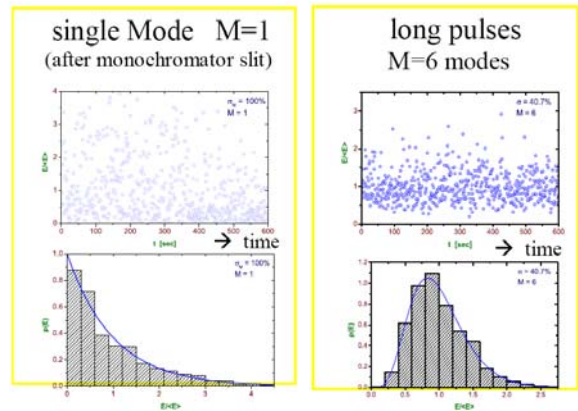


Figure 7: Pulse-to-pulse fluctuation of SASE pulse energy for different settings of the FLASH electron bunch length. Upper row: measured single pulse energy versus time; lower row: histogram of probability distribution extracted from the measurement. The SASE pulses are observed at high gain, but still in the exponential regime, not yet in saturation. The plots on the left hand side illustrate the case of a single mode which can be realized, for instance, by accepting only the radiation that has passed a monochromator slit, thus making the wave longer than the bunch.

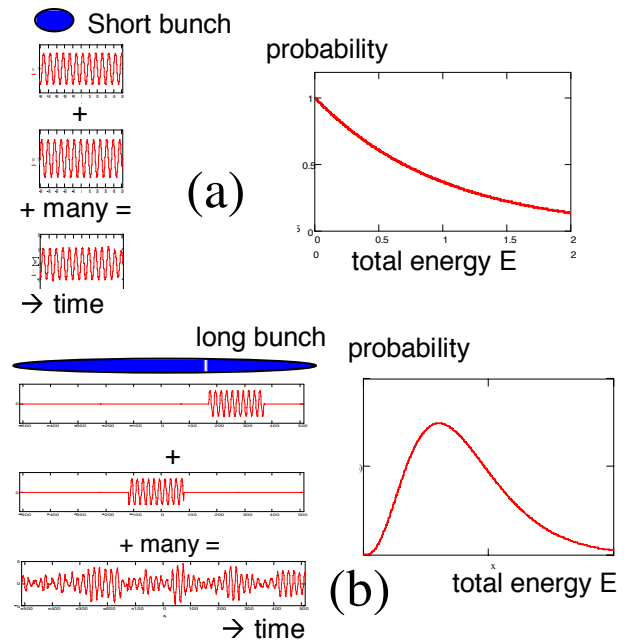


Figure 8: A simple model for statistical properties of superposition of many wave trains originating from individual electrons. See text.

According to statistical optics, the resulting probability distribution function is given by a Gamma distribution [12,13]:

$$g_M(E) \cdot dE \propto \frac{1}{\Gamma(M)} (E)^{M-1} e^{-E} \cdot dE$$

Analysis of the experimentally determined intensity fluctuation thus provides important information: If it agrees with a Gamma distribution, we know that the FEL operates in the regime of exponential growth (no saturation yet), and we can extract the parameter M providing information about the typical pulse length: $\tau_L \approx M \cdot \lambda_{\text{coh}}$. Note that λ_{coh} is determined by the measured bandwidth of the radiation spectrum, and by the measured gain length.

Finally it is important to realize that complementary information about the pulse length and the number of modes is provided from the width and number of spikes, respectively, observed in single shot spectra of radiation pulses, see Fig. 9. At FLASH (see Fig. 5) this analysis results in an estimated pulse length of ~ 10 fs and less than two modes in average, in agreement with predictions of start-to-end beam dynamics calculation of the electron beam. It should be noted that if the assumption of full transverse coherence made here is not valid, more modes will show up that do not contribute to the pulse length.

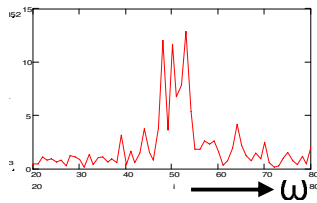


Figure 9: Fourier transform of the time signal shown in the bottom plot of Fig. 8. The envelope width of the resonance curve corresponds to the coherence length while the width of the individual spikes corresponds to the length of the entire signal.

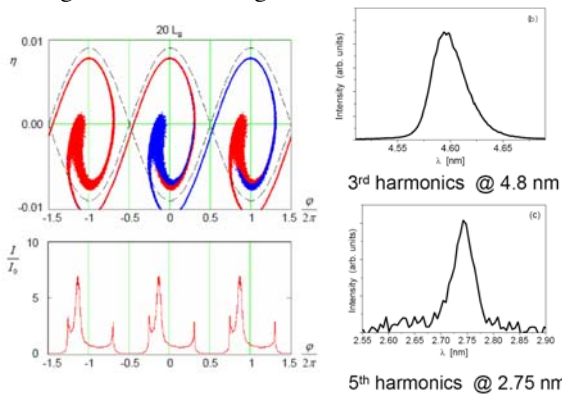


Figure 10: upper left part: Phase space distribution after ca. 18 power gain lengths. Lower left part: longitudinal charge density distribution possessing pronounced higher Fourier harmonics. Right: Higher harmonics observed in the FLASH pulse spectrum [8].

TRANSVERSE COHERENCE

It is well known that a Gaussian optical beam with perfect transverse coherence has transverse emittance $\varepsilon_{\text{Light}} = \sigma_r \cdot \sigma_\theta = \lambda_{\text{Light}} / 4\pi$. It is thus not surprising that FEL theory expects a large degree of transverse coherence of the output beam if the electron beam has an emittance

$\varepsilon_{\text{electrons}} \leq \lambda_{\text{Light}} / 4\pi$. This has in fact been verified at FLASH for wavelengths 32, 25 and 13 nm [11, 14].

HARMONICS

While the longitudinal density modulation described in Section 2 is rather sinusoidal within the initial part of the gain process, further motion in the $\Delta\gamma/\Psi$ phase plane results in considerable higher harmonics of the charge density, thus driving, in turn, higher harmonics of the radiation if the FEL enters the saturation regime, see Fig. 10.

CONCLUSION

Within the established theory of SASE FELs, all the radiation characteristics observed so far can be explained by electron beam parameters at the entrance of the undulator in a way consistent with results of state-of-the-art beam dynamics simulation and electron beam diagnostics. While impressive progress in these latter fields has been made [15,16] it is not yet possible to either model or measure the electron beam properties at such precision that the FEL radiation can be predicted at sufficient precision. In particular in view of X-ray FELs being under way, there is thus good reason to support even more refined beam dynamics investigations as well as precise beam diagnostics with Femtosecond resolution.

ACKNOWLEDGEMENT

The author acknowledges numerous discussions with his colleagues E.L. Saldin, E.A. Schneidmiller, and M.V. Yurkov, and the collaboration with the entire FLASH team.

REFERENCES

- [1] J.M.J. Madey, J Appl. Phys. **42**, 1906 (1971)
- [2] E.L. Saldin, E.A. Schneidmiller, M.V. Yurkov, *The Physics of Free-Electron Lasers* (Springer, 1999).
- [3] J. Rossbach, CERN Accelerator School, Brunnen, CERN-2005-012 (2005).
- [4] R. Bonifacio, C. Pellegrini, L.M. Narducci, Opt. Commun. **50**, 373 (1984).
- [5] K.J. Kim, Phys. Rev. Lett. **57**, 1871 (1986)
- [6] A. Murokh, et al., Proc. 2001 Part. Acc. Conf. (2001)
- [7] S. Milton et al, Science **292**, 2037 (2001)
- [8] W. Ackermann, et al., nature photonics **1**, 336 (2007)
- [9] E.L. Saldin, E.A. Schneidmiller, M.V. Yurkov, Nucl. Instr. Meth. **A429**, 233 (1999)
- [10] A.M. Kondratenko, E.L. Saldin, Part. Accelerators **10**, 207 (1980)
- [11] V. Ayvazyan et al., Phys. Rev. Lett. **88**, No.10 (2002)
- [12] J. Goodman, *Statistical Optics*, Wiley, (1995)
- [13] E.L.Saldin, E.A. Schneidmiller, M.V. Yurkov, Opt. Commun. **148**, 383 (1998)
- [14] I. Vartanyants, et al., HASYLAB Annual Report 2006 Part I, 207 (2006)
- [15] M. Roehrs, this conference
- [16] O. Grimm, this conference